Indeterminate Multi-Point Impact with Friction of Agile Legged Robots

Adrian Rodriguez and Alan Bowling

***Abstract*— This work presents an analysis of the simultaneous, multiple point impact forces on an agile legged robot. An analytic solution is developed for determining the system's post impact dynamic behavior. A discrete, algebraic model is used with an event-driven function which finds impact events. The indeterminate nature of the system equations of motion encountered at impact is addressed with the implementation of a constraint equation. An algorithm that is based on an analytic approach and an energetic COR is used to resolve the post impact velocities of the system. A simple planar model of a ball is considered for the leg's foot and a simulation is presented to demonstrate the effectiveness of the proposed approach.**

I. INTRODUCTION

The analysis of agile legged robots involves the examination of the impact forces these systems experience in an environment. The determination of the impact forces is important because it defines the robot's agility, or ability to quickly change direction when its legs impact the ground. It is common for multiple contacts to occur at each foot of these legged systems, which introduces equations of motion that are indeterminate with respect to the impact forces. This paper introduces a method for obtaining an analytic solution of a system undergoing multiple, simultaneous impact with friction. The analytic approach and formulation developed in previous work for planar impact of a single point, [1], is modified here to account for multiple point, simultaneous impact of a single body. The principles of the work-energy theorem are applied and an energetic coefficient of restitution (COR) is used for the collision to ensure energy consistency.

For the purposes of this analysis, a simple test case is considered to study the ground-contact interaction of a leg's foot with its environment and to evaluate the effectiveness of the proposed approach. Thus, a planar model of a ball which undergoes multiple impact points is examined. The ball, shown in Fig. 1 with radius R, has three degrees-of-freedom (DOFs) denoted by generalized coordinates q_1 and q_2 which are translational and q_3 which is rotational. The ball's position is indicated by the position vector $\mathbf{P_{NO}}$. At the point of impact, the ball is in simultaneous contact with the ground, point 1, and the wall, point 2. Two force components are present at each impact point, as shown in Fig. 1. One force is normal to both surfaces and the other is tangential to both surfaces, caused by friction.

A. Rodriguez is with the Department of Mechanical and Aerospace Engineering, University of Texas at Arlington, Arlington, TX 76017 USA adrianrodriguez2009@mavs.uta.edu

A. Bowling is with the Department of Mechanical and Aerospace Engineering, University of Texas at Arlington, Arlington, TX 76017, USA bowling@uta.edu

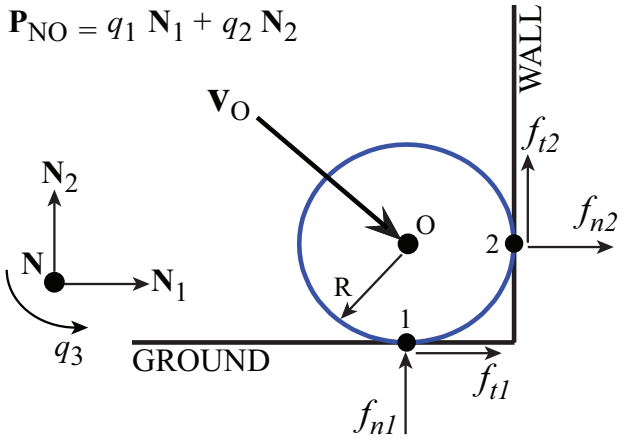

Fig. 1. Planar model of a ball with forces at the impact points.

The remainder of the paper is organized as follows. Background will be presented on the methods used to treat the rigid body collision considered in this work. Then, a brief discussion of the method used to address the indeterminacy of the equations of motion followed by the algorithm developed for the analytic approach which considers multiple, simultaneous impact with friction will be presented. The paper will end with simulation results of the model considered and meaningful conclusions drawn from this work.

II. BACKGROUND

Classical rigid body collision theory has been extensively used to study and treat multiple point impact with friction [2], [3], [4]. The continuous and discontinuous methods are the two common approaches used to examine rigid body impact. In this work, a discontinuous approach is used which splits the impact event into two regions: before and after impact. This approach assumes that the impact event occurs over a very short time period in which the position and orientation of the system remains constant [5]. The detection of an impact is captured using an event function in conjunction with Matlab's ode45.m integrator. The simulation is stopped, and the post impact generalized speeds are calculated and updated before restarting the simulation.

Dynamic modeling of systems involving simultaneous, multiple impacts with friction yield equations of motion which are indeterminate with respect to the impact forces [2], [6], [7], [8]. This indeterminacy is caused by a non-square Jacobian, which is not invertible, and premultiplies the impact forces in the equations of motion. This is problematic because the impact forces are needed to determine the state

of sticking or slipping at each impact point. There are methods available which have been used in the literature for addressing this situation.

One simple method is to add more degrees-of-freedom to the problem by considering elasticity in the bodies [2]. This is in contrast to rigid body approaches, which directly consider the properties of the non-square Jacobian. Other techniques for addressing the indeterminacy of the equations involve the use of QR factorization techniques [6] or eliminate infeasible solutions to the contact forces [7], [8].

Based on the hard impact modeling used here, it is possible to define a relationship, or constraint, among the velocities of the impact points on the rigid body. The constraints developed in [9] are more consistent with the assumptions which form the basis for classical rigid body impact analysis, in contrast to [6]. The dual nature of the impact Jacobian, which expresses a relationship between velocities and forces, can be used to redefine the constraint in terms of forces.

The rigid body collisions examined in this work are treated as hard impacts within the framework of a discrete model. Any deformations that occur between the impacting bodies are considered to be very small and are neglected. An algebraic approach to discrete modeling defines enough equations to describe the system such that the post impact velocities can be solved algebraically [10], [11]. These velocities dictate the behavior of the system after impact.

The underlying theory governing approaches for resolving the post impact velocities are based on the classical hypotheses of Newton, Poisson, and Stronge which have been extensively used to study rigid body collisions [12], [1], [2]. Each classical hypothesis uniquely defines a coefficient of restitution and are commonly used to examine hard impacts.

A discrete, algebraic method is used in this work to treat rigid body impacts. Unlike other algebraic approaches, an optimization is not used here to resolve the velocities nor does a complementarity problem need to be solved. The approach and methods used here are most similar to [1], in which a analytic solution to the problem is obtained.

A different formulation than in [1] is developed and modified in this work to address simultaneous, multi-point collision with friction. An energetic coefficient of restitution (COR) according to Stronge's hypothesis [13] is used which makes use of the work-energy theorem as in [14]. The work-energy theorem examines the mechanical energy of the system during the compression and restitution phases of the impact and relates it to the work done on the system. This provides the basis for obtaining an analytical solution that is both unique and energetically consistent.

III. CONSTRAINT EQUATION

Examination of the impulse forces requires consideration of the impact forces in the equations of motion,

$$A\,\ddot{\mathbf{q}} + \mathbf{g}(\mathbf{q}) \;=\; \mathbf{\Gamma}(\mathbf{q}) \;=\; J^T(\mathbf{q})\;\mathbf{F} \tag{1}$$

where A is the mass matrix, $\mathbf{\Gamma}$ contains the generalized active forces, and J is a Jacobian matrix that defines the velocity and forces at the impact points. The generalized coordinates and accelerations are included in $\mathbf{q}$ and $\ddot{\mathbf{q}}$, while $\mathbf{g}$ and $\mathbf{F}$ are vectors of gravity and impact forces, respectively.

For the ball considered in this work, the equations of motion take the form of,

$$A \begin{bmatrix} \ddot{q}_1 \\ \ddot{q}_2 \\ \ddot{q}_3 \end{bmatrix} + \mathbf{g}(\mathbf{q}) \;=\; \mathbf{\Gamma}(\mathbf{q}) \;=\; J^T \begin{bmatrix} f_{t1} \\ f_{n1} \\ f_{t2} \\ f_{n2} \end{bmatrix} \tag{2}$$

This gives three equations but four unknown forces defined by f_{t1}, f_{n1}, f_{t2}, and f_{n2}, resulting in equations which are indeterminate with respect to these impact forces.

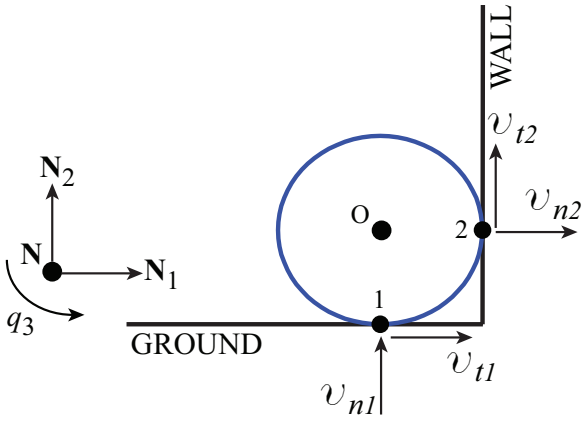

Fig. 2. Normal and tangential velocities at the impact points.

In [9], velocity constraints consistent with rigid body dynamics were defined to address the indeterminacy in (2). A similar velocity constraint for the planar model considered in Fig. 2 can be derived and expressed as,

$$v_{n1} + v_{t1} - v_{t2} - v_{n2} = 0 \tag{3}$$

which are the velocity components at the impact points, shown in Fig. 2. The duality of the impact Jacobian expresses a relationship between velocities and forces, shown as

$$\boldsymbol{\vartheta} = \begin{bmatrix} v_{t1} \\ v_{n1} \\ v_{t2} \\ v_{n2} \end{bmatrix} = J\;\dot{\mathbf{q}}\;, \qquad \mathbf{\Gamma} = J^T\;\mathbf{F} = J^T \begin{bmatrix} f_{t1} \\ f_{n1} \\ f_{t2} \\ f_{n2} \end{bmatrix} \tag{4}$$

can be applied to (3) such that the constraint becomes,

$$f_{n1} + f_{t1} - f_{t2} - f_{n2} = 0 \tag{5}$$

The integration of the impact forces during a short impact event ϵ is defined as [15],

$$\int_t^{t+\epsilon} \mathbf{F}\;dt = \mathbf{p} = \begin{bmatrix} p_{t1} \\ p_{n1} \\ p_{t2} \\ p_{n2} \end{bmatrix} \tag{6}$$

such that the definite integration of (5) over a short time period gives the constraint in terms of impulses,

$$p_{n1} + p_{t1} - p_{t2} - p_{n2} = 0 \tag{7}$$

The expression in (7) will serve as the additional equation needed to address the indeterminacy in the equations of motion. The analytic solution and the alogorithm used to find the post impact velocities will be presented in Sec. IV.

IV. ANALYTIC APPROACH

In this section, the analytic solution proposed in this work will be explained. The equations of motion will first be rewritten and expressed in terms of a normal impulse parameter. Then, the method used to calculate the normal work for the collision will be presented.

A. Equations of motion

The equations of motion are revisited and a definite integration of (2) over a short time ϵ for the impact event,

$$\int_t^{t+\epsilon} (A\ \ddot{\mathbf{q}} + \mathbf{g}\ (\mathbf{q}))\ dt = \int_t^{t+\epsilon} J^T(\mathbf{q})\ \mathbf{F}\ dt \tag{8}$$

gives,

$$A\ (\ \dot{\mathbf{q}}(t+\epsilon) - \dot{\mathbf{q}}(t)\ ) = J^T\mathbf{p} \tag{9}$$

It should be noted that for the modeling of a legged robot, which consists of a multi-body system, internal forces and torques would be present in the equations of motion. Although, these forces would be considered very small and negligible compared to the magnitude of the impulse forces after integration of the equations over the short impact event. Hence, it is appropriate to continue this analysis for the test case considered in Fig. 1.

Multiplying the inverse of the mass matrix on each side of (9) and using $\triangle\dot{\mathbf{q}}$ to represent the change between pre- and post-impact generalized speeds,

$$\triangle\dot{\mathbf{q}} = A^{-1}J^T\mathbf{p} = \mathrm{L}\ \mathbf{p} = [\mathbf{L}_{t1} \mid \mathbf{L}_{n1} \mid \mathbf{L}_{t2} \mid \mathbf{L}_{n2}]\ \mathbf{p} \tag{10}$$

where $\mathrm{L} \in \Re^{3X4}$ can be termed as a collision matrix. The columns of L are shown to uncover their respective normal and tangential contributions as column vectors.

Finally, the product can be carried out such that the equations of motion take the form of,

$$\triangle\dot{\mathbf{q}} = \mathbf{L}_{t1}\ p_{t1} + \mathbf{L}_{n1}\ p_{n1} + \mathbf{L}_{t2}\ p_{t2} + \mathbf{L}_{n2}\ p_{n2} \tag{11}$$

In this work, Coulomb friction is used to characterize the relationship between normal and tangential forces using a coefficient of friction μ,

$$f_t = \pm\mu\ |f_n| \tag{12}$$

where the sign in (12) will depend on the direction of friction at the impact point. Given that the method used here considers the impulses at impact, (12) can be expressed in terms of impulses as in [16], [17] after a definite integration,

$$p_t = \pm\mu\ |p_n| \tag{13}$$

An expression for the tangential impulses at each impact point using Coulomb's friction can be written for the model illustrated in Fig. 1 as,

$$p_{t1} = \pm\mu_1\ |p_{n1}| \qquad p_{t2} = \pm\mu_2\ |p_{n2}| \tag{14}$$

The point at which no-slip occurs at the ground and wall impact points can be indicated by $v_{t1} = 0$ and $v_{t2} = 0$, respectively. Using Coulomb friction, the tangential impulses for no-slip can be expressed as,

$$p_{t1} = m_1\ |p_{n1}| \qquad p_{t2} = m_2\ |p_{n2}| \tag{15}$$

where $m_1, m_2 \leq \mu_s$. The terms m_1, m_2 are coefficients of friction for no-slip and μ_s is the static coefficient of friction.

The specific model considered in Fig. 1 will be treated with the theory developed here, which uses (11) and (14) without any loss of generality. The absolute value of the normal impulse terms in (11) can be taken while preserving their signs and the expressions in (14) can be substituted into (11) to give,

$$\begin{aligned}\triangle\dot{\mathbf{q}} = \mathbf{L}_{t1}(\pm\mu_1|p_{n1}|) + \mathbf{L}_{n1}(|p_{n1}|) \\ +\mathbf{L}_{t2}(\pm\mu_2|p_{n2}|) + \mathbf{L}_{n2}(-|p_{n2}|)\end{aligned} \tag{16}$$

where the sign of the tangential terms are kept ambiguous and will depend on the direction of friction acting at each impact point. The two normal impulse terms in (16) can be collected to obtain,

$$\triangle\dot{\mathbf{q}} = (\mathbf{L}_{n1} \pm \mu_1\mathbf{L}_{t1})\ |p_{n1}| + (-\mathbf{L}_{n2} \pm \mu_2\mathbf{L}_{t2})\ |p_{n2}| \tag{17}$$

Furthermore, the constraint equation obtained in (7) can be rewritten to include the Coulomb friction expressions in (14) and the magnitudes of the normal impulse terms.

$$|p_{n1}| \pm \mu_1|p_{n1}| \pm \mu_2|p_{n2}| + |p_{n2}| = 0 \tag{18}$$

This constraint equation will be used to eliminate one of the normal impulse terms in (17). There is no rationale for selecting which term to eliminate but here and througout the remaining section $|p_{n2}|$ has been removed, such that

$$\begin{aligned}\triangle\dot{\mathbf{q}} &= [(\mathbf{L}_{n1} \pm \mu_1\mathbf{L}_{t1}) + \mu_{12}(-\mathbf{L}_{n2} \pm \mu_2\mathbf{L}_{t2})]\ |p_{n1}| \\ &= (\mathbf{L}_1 + \mu_{12}\mathbf{L}_2)|p_{n1}|\end{aligned} \tag{19}$$

where,

$$\mu_{12} = -\frac{(1 \pm \mu_1)}{(1 \pm \mu_2)} \tag{20}$$

The expression in (19) describes the dependence of the post impact generalized speeds in $\dot{\mathbf{q}}$ on the normal impulse, $|p_{n1}|$, since $\triangle\dot{\mathbf{q}} = \dot{\mathbf{q}} - \dot{\mathbf{q}}_o$.

Recall from (4) the relationship between the velocities at the impact points in $\boldsymbol{\vartheta}$ and the generalized speeds in $\dot{\mathbf{q}}$, such that the left-hand side of (19) can be written as,

$$\begin{aligned}\triangle\dot{\mathbf{q}}\ &= \dot{\mathbf{q}} - \dot{\mathbf{q}}_o = (J^TJ)^{-1}J^TJ(\dot{\mathbf{q}} - \dot{\mathbf{q}}_o) \\ &= (J^TJ)^{-1}J^T(\boldsymbol{\vartheta} - \boldsymbol{\vartheta}_o) \\ &= J^*(\boldsymbol{\vartheta} - \boldsymbol{\vartheta}_o)\end{aligned} \tag{21}$$

Equating (21) back with the right-hand side of (19) yields,

$$J^*(\boldsymbol{\vartheta} - \boldsymbol{\vartheta}_o) = (\mathbf{L}_1 + \mu_{12}\mathbf{L}_2)|p_{n1}| \tag{22}$$

where it is more clear to see the effect of $|p_{n1}|$ on the normal velocities contained in $\boldsymbol{\vartheta}$. In this way, the calculation of the normal work will be derived for the application of Stronge's hypothesis which will be discussed in the following section.

B. Energy exchange at impact: Work-Energy Theorem

Here, the derivation of the normal work resulting from the rigid body collision will be developed. As it was noted earlier, an energetic COR according to Stronge's hypothesis [13] is used in this work to treat the impact.

Stronge's hypothesis incorporates the work-energy theorem by relating the normal work between the compression and restitution phases of the collision. The work-energy theorem defines that the sum of the final kinetic, T_f, and potential, U_f, energy of a system is given by the sum of the initial kinetic, T_o, and potential, U_o, energy plus the work done, W, to get to the final state. This can be written for the rigid body collision considered here as,

$$T_f = T_o + W \tag{23}$$

where the potential energy terms have been neglected due to the hard impact modeling used. The calculation of the work is given as the change in kinetic energy between the final and inital states of the collision as,

$$W = T_f - T_o = \frac{1}{2}\dot{\mathbf{q}}^T A\ \dot{\mathbf{q}} - \frac{1}{2}\dot{\mathbf{q}}_o^T A\ \dot{\mathbf{q}}_o \tag{24}$$

By using the same representation of the generalized speeds $\dot{\mathbf{q}}$ and $\dot{\mathbf{q}}_o$ in (21), then (24) can be expressed as,

$$W = \frac{1}{2}(J^*\boldsymbol{\vartheta})^T A\ (J^*\boldsymbol{\vartheta}) - \frac{1}{2}(J^*\boldsymbol{\vartheta}_o)^T A\ (J^*\boldsymbol{\vartheta}_o) \tag{25}$$

where the velocities at the impact points in $\boldsymbol{\vartheta}$ and $\boldsymbol{\vartheta}_o$ can be realized in the calculation of the work.

Stronge's hypothesis only considers the normal work done during a collision which is a function of the velocities normal to each impact point. To capture the effects that the right hand side of (25) has on the normal work due to the normal velocities, then a distinction must be made between the contributing and non-contributing parts.

If the term J^* is split into column vectors and represented as $J^* = [\mathbf{J}_1^*|\mathbf{J}_2^*|\mathbf{J}_3^*|\mathbf{J}_4^*]$, then the product of these vectors with the velocity components in (25) yields,

$$\begin{aligned} W = &\frac{1}{2}\left(\mathbf{J}_t^*\boldsymbol{\vartheta}_t + \mathbf{J}_n^*\boldsymbol{\vartheta}_n\right)^T A\ \left(\mathbf{J}_t^*\boldsymbol{\vartheta}_t + \mathbf{J}_n^*\boldsymbol{\vartheta}_n\right) \\ &-\frac{1}{2}\left(\mathbf{J}_t^*\boldsymbol{\vartheta}_{to} + \mathbf{J}_n^*\boldsymbol{\vartheta}_{no}\right)^T A\ \left(\mathbf{J}_t^*\boldsymbol{\vartheta}_{to} + \mathbf{J}_n^*\boldsymbol{\vartheta}_{no}\right) \end{aligned} \tag{26}$$

where $\mathbf{J}_t^* = [\mathbf{J}_1^*|\mathbf{J}_3^*]$ and $\mathbf{J}_n^* = [\mathbf{J}_2^*|\mathbf{J}_4^*]$. The normal and tangential velocity components in (26) are distinguished by the terms $\boldsymbol{\vartheta}_t = [v_{t1}|v_{t2}]^T$ and $\boldsymbol{\vartheta}_n = [v_{n1}|v_{n2}]^T$, respectively.

The product of the terms in (26) can be carried out to determine the position of the normal velocity terms with respect to the tangential terms so that only the parts contributing to the normal work can be extracted.

$$\begin{aligned} W = &\frac{1}{2}(\boldsymbol{\vartheta}_t^T\mathbf{J}_t^{*T} A\ \mathbf{J}_t^*\boldsymbol{\vartheta}_t + 2\ \boldsymbol{\vartheta}_t^T\mathbf{J}_t^{*T} A\ \mathbf{J}_n^*\boldsymbol{\vartheta}_n \\ &+\boldsymbol{\vartheta}_n^T\mathbf{J}_n^{*T} A\ \mathbf{J}_n^*\boldsymbol{\vartheta}_n) - \frac{1}{2}(\boldsymbol{\vartheta}_{t_o}^T\mathbf{J}_t^{*T} A\ \mathbf{J}_t^*\boldsymbol{\vartheta}_{to} \\ &+2\ \boldsymbol{\vartheta}_{t_o}^T\mathbf{J}_t^{*T} A\ \mathbf{J}_n^*\boldsymbol{\vartheta}_{no} + \boldsymbol{\vartheta}_{n_o}^T\mathbf{J}_n^{*T} A\ \mathbf{J}_n^*\boldsymbol{\vartheta}_{no}) \end{aligned} \tag{27}$$

A careful look at all the parts in (27) shows tangential, normal, and coupled tangential and normal parts due to the multiple point impact modeling, and are indicated by the $\boldsymbol{\vartheta}_t$ and $\boldsymbol{\vartheta}_n$ terms. As it was stated earlier, the velocities normal to the impact points are the primary source to the normal work done in a collision. Thus, if the tangential parts are neglected and only the parts that are a function of the normal velocities, in $\boldsymbol{\vartheta}_n$, are considered, then the normal work can be expressed as,

$$\begin{aligned} W_n = &\boldsymbol{\vartheta}_t^T\mathbf{J}_t^{*T} A\ \mathbf{J}_n^*\boldsymbol{\vartheta}_n + \frac{1}{2}\boldsymbol{\vartheta}_n^T\mathbf{J}_n^{*T} A\ \mathbf{J}_n^*\boldsymbol{\vartheta}_n \\ &-(\boldsymbol{\vartheta}_{t_o}^T\mathbf{J}_t^{*T} A\ \mathbf{J}_n^*\boldsymbol{\vartheta}_{no} + \frac{1}{2}\boldsymbol{\vartheta}_{n_o}^T\mathbf{J}_n^{*T} A\ \mathbf{J}_n^*\boldsymbol{\vartheta}_{no}) \end{aligned} \tag{28}$$

A plot of the normal work for a rigid body collision reveals its quadratic nature as a function of $|p_n|$. The minima of the curve, at $|p_{nc}|$, marks the end of the work done in the compression phase, W_{nc}, and the start of the restitution phase. This can be solved for by differentiating (28) with respect to the normal impulse, $|p_{n1}|$, and equating it to zero.

The net normal work, W_{nf}, at the end of the collision is determined using Stronge's hypothesis, defined as [13],

$$e_*^2 = -\frac{W_{nr}}{W_{nc}} = -\frac{W_{nf} - W_{nc}}{W_{nc}} \tag{29}$$

such that,

$$W_{nf} = W_{nc}(1 - e_*^2) \tag{30}$$

where $0 \leq e_* \leq 1$ and W_{nr} is the normal work during the restitution phase of the collision. The normal impulse, $|p_{nf}|$, signifies the end condition for the collision and can be determined once W_{nf} is known.

V. RESOLVING POST IMPACT VELOCITIES

In Sec. IV-B, an expression for the normal work during the collision was determined and will be used to resolve the post impact velocities of the system. The first step in the algorithm is to intuitively determine the friction direction of the impact points based on the pre-impact tangential velocities. This allows for the sign conventions presented in (19) to be defined.

The next step is to evaluate the order in which each velocity component, among those illustrated in Fig. 2, reaches a value of zero. This is accomplished by calculating the value of the normal impulse during the collision that is needed to drive each velocity component to zero.

Recall (19), where the equations of motion were expressed in terms of the normal impulse, $|p_{n1}|$. Multiplying each side by the impact Jacobian to express the generalized speeds as velocities of the impact points, as in (4) gives,

$$J\triangle\dot{\mathbf{q}} = \begin{bmatrix} v_{t1} \\ v_{n1} \\ v_{t2} \\ v_{n2} \end{bmatrix} - \begin{bmatrix} v_{t1} \\ v_{n1} \\ v_{t2} \\ v_{n2} \end{bmatrix}_o = J(\mathbf{L}_1 + \mu_{12}\mathbf{L}_2)\ |p_{n1}| \tag{31}$$

where projections of $|p_{n1}|$ that drive the velocities of the impact points to zero can be calculated.

In the event that a tangential velocity reaches zero before $|p_{nc}|$ is reached in the collision, then the impact point is examined to determine if slip or no-slip occurs, which is

governed by the static coefficient of friction. If slipping occurs, then the friction direction changes such that the sign in (19) is reversed for that impact point. In the case of no-slip, then the coefficient of friction for a tangential velocity of zero, $m_i \in i = 1, 2$ is used in (16).

The change of signs in (19) cause a shift in the W_n vs. $|p_{n1}|$ plot and updated values for the normal impulse contributions must be calculated for the remaining velocity components. After $|p_{nc}|$ is reached in the colllision, then the net normal work, W_{nf}, can be calculated using the energetic COR. Lastly, the end condition for the normal impulse, $|p_{nf}|$, is evaluated to allow for the calculation of the post impact velocities using (31).

VI. RESULTS

Here, a simulation of a ball impacting a corner, as in Fig. 1, is performed for a planar case to show that the proposed method yields an analytic and energetically consistent solution for the post impact velocities. A static and dynamic coefficient of friction of 0.5 and 0.25 is used for the impacting surfaces.

TABLE I

MODEL STATES THROUGHOUT THE COLLISION.

	Initial	Pre-impact	Post impact
Position			
q_1	0.000 m	3.614 m	3.614 m
q_2	1.500 m	0.500 m	0.500 m
q_3	0.000 rad	0.000 rad	0.000 rad
Velocity			
$\dot{q}_1$	8.000 m/s	8.000 m/s	-3.004 m/s
$\dot{q}_2$	0.000 m/s	-4.430 m/s	3.832 m/s
$\dot{q}_3$	0.000 m/s	0.000 m/s	-5.178 m/s

The initial, pre-impact, and post impact states of the ball are presented in Table I. The simulation was started with some initial conditions and the remaining states were determined from the application of the algorithm discussed in Sec. V for the rigid body collision.

A plot of the normal work throughout the collision is shown in Fig. 3. There are two apparent shifts in the normal work curve which occur at the points where $v_{t2} = 0$ and $v_{t1} = 0$. At the instance where each tangential velocity reaches zero, the slip-state of the impact point is evaluated to determine if it is in a state of slip or no-slip, which is governed by the static coefficient of friction.

The importance of knowing where the tangential velocities cross zero was noted in Sec. V because they dictate changes in the velocity trajectories and normal work during the compression phase of the collision. Each tangential velocity crosses zero in the compression phase and in both cases, the impact points were in a state of slipping during the collision, which resulted in a reversal of the friction direction at the impact point causing the shifts in the normal work plot. The effects of the change in friction direction are also experienced in the trajectories of the velocities, as seen in Fig. 4.

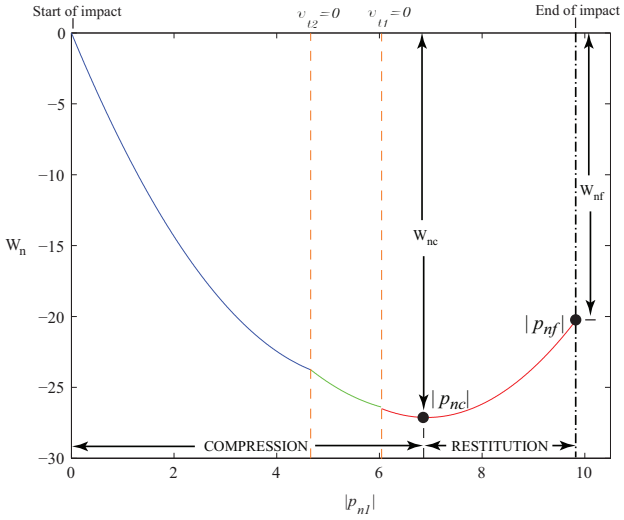

Fig. 3. Normal work done throughout the collision.

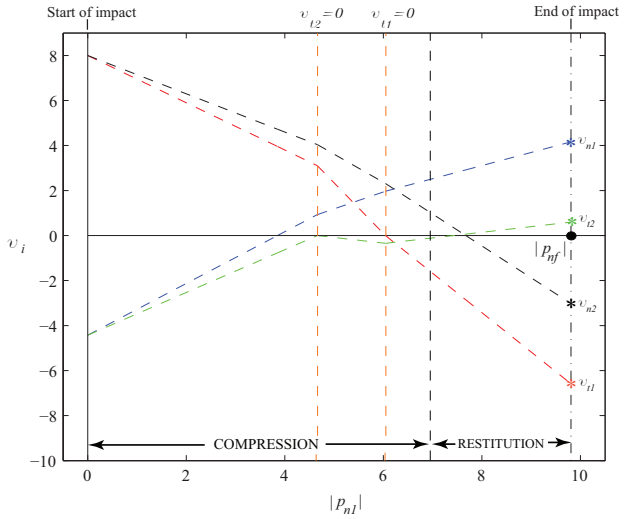

Fig. 4. Velocity trajectories throughout the collision.

Once the collision reaches $|p_{nc}|$ and the amount of normal work done during the compression phase is determined, then the application of Stronge's hypothesis gives the net normal work, W_{nf}, at the end of the collision. The end condition for the normal impulse, $|p_{nf}|$, is evaluated with the knowledge of W_{nf}, which marks the end of the collision. Lastly, the post impact generalized speeds are calculated using (31), as shown in Fig. 4, which serve as the initial conditions for restarting the numerical integration to simulate the system after impact.

The simulation of the ball is depicted as it impacts a corner defined by the ground and a wall and ends when a second impact is captured with the ground, as shown in Fig. 5. The ball has no angular velocity prior to impact but a negative angular velocity after impact. This angular velocity is attributed to the tangential velocity at the wall reaching zero prior to the tangential velocity at the ground impact point. The trajectory of the ball's mass center throughout

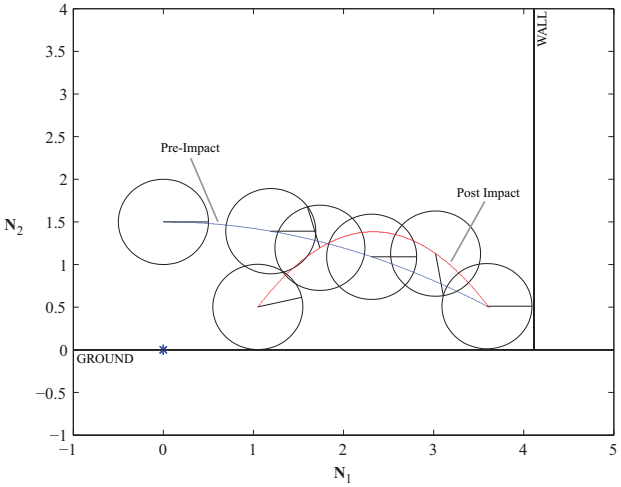

Fig. 5. Simulation results for the rigid body collision.

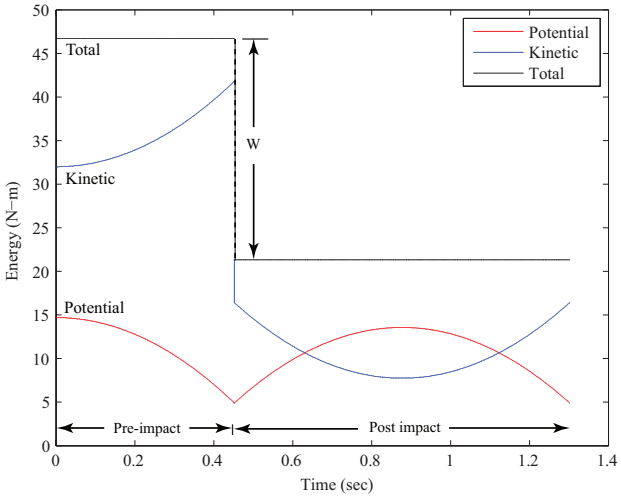

Fig. 6. Energy consistency throughout the simulation.

the simulation, as shown in Fig. 5, demonstrates that the ball followed a higher trajectory after impact due to the velocities determined at the end of the collision. The final position of the system in the simulation lies before its intial position indicating some loss of energy.

A plot of the potential, kinetic, and total energy of the system throughout the simulation is shown in Fig. 6. The total energy lost due to impact corresponds with the amount of total net work, W, at the end of the collision, as calculated from (27). The net normal work, W_n, given by the results shown in Fig. 3 is consistent with the calculation of W, where the remaining losses can be attributed to tangential work. The consistency among the results in Fig. 3 and Fig. 6 validates the methods used to treat the rigid body collision.

VII. CONCLUSIONS

In this work, a simple planar model of a ball which undergoes simultaneous, multi-point impact with friction was examined for the analysis of an agile legged robot. A constraint equation was derived in terms of impulses to address the indeterminacy of the equations of motion and served as an additional equation for the discrete, algebraic model considered here. It was shown that the proposed approach, which makes use of an energetic COR, led to the determination of an analytical solution for the post impact generalized speeds of the system. It was also shown that the solution was energetically consistent by the methods used to treat the rigid body collision and examining the system's total energy throughout the simulation.

REFERENCES

[1] S. Djerassi, "Stronge's hypothesis-based solution to the planar collision-with-friction problem," *Multibody System Dynamics*, vol. 24, no. 4, pp. 493–515, Dec. 2010.

[2] Y. Wang, V. Kumar, and J. Abel, "Dynamics of rigid bodies undergoing multiple frictional contacts," *Proceedings-IEEE International Conference on Robotics and Automation*, vol. 3, pp. 2764–2769, May 1992.

[3] L. Johansson, "A linear complementarity algorithm for rigid body impact with friction," *European Journal of Mechanics, A/Solids*, vol. 18, no. 4, pp. 703–717, Jul. 1999.

[4] D. Stewart, "Rigid-body dynamics with friction and impact," *SIAM Review*, vol. 42, no. 1, pp. 3–39, Mar. 2000.

[5] G. Gilardi and I. Sharf, "Literature survey of contact dynamics modelling," *Mechanism and Machine Theory*, vol. 37, no. 10, pp. 1213–1239, Oct. 2002.

[6] L. Johansson, "A Newton method for rigid body frictional impact with multiple simultaneous impact points," *Computer Methods in Applied Mechanics Engineering*, vol. 191, pp. 239–254, Nov. 2001.

[7] Y. Maeda, K. Oda, and S. Makita, "Analysis of indeterminate contact forces in robotic grasping and contact tasks," *IEEE Int'l Conference on Intelligent Robots and Systems*, pp. 1570–1575, Oct. 2007.

[8] T. Omata and K. Nagata, "Rigid body analysis of the indeterminate grasp force in power grasps," *IEEE Transactions on Robotics and Automation*, vol. 16, no. 1, pp. 46–54, Feb. 2000.

[9] A. Rodriguez and A. Bowling, "Indeterminate impact and contact with friction," *Multibody System Dynamics (In Review)*.

[10] B. Brogliato, A. Ten Dam, and et al., "Numerical simulation of finite dimensional multibody nonsmooth mechanical systems," *App. Mech. Reviews*, vol. 55, no. 2, pp. 107–149, Mar. 2002.

[11] A. Bowling, D. Flickinger, and et al., "Energetically consistent simulation of simultaneous impacts and contacts in multibody systems with friction," *Multibody Sys Dyn*, vol. 22, no. 1, pp. 27–45, Aug. 2009.

[12] S. Djerassi, "Collision with friction; part A: Newton's hypothesis," *Multibody Sys Dyn*, vol. 21, no. 1, pp. 37–54, Feb. 2009.

[13] W. Stronge, *Impact Mechanics*. Cambridge University Press, 2000.

[14] P. Bergés and A. Bowling, "Rebound, slip, and compliance in the modeling and analysis of discrete impacts in legged locomotion," *Journal of Vibration and Control*, vol. 17, no. 12, pp. 1407–1430, Dec. 2006.

[15] A. Bedford and W. Fowler, *Engineering Mechanics: Dynamics*. Pearson Education, Inc., 2008.

[16] I. Han and B. Gilmore, "Multi-body impact motion with friction-analysis, simulation, and experimental validation," *Journ/Mechl Design, Trans. of the ASME*, vol. 115, no. 3, pp. 412–422, Sep. 1993.

[17] D. Flickinger and A. Bowling, "Simultaneous oblique impacts and contacts in multibody systems with friction," *Multibody System Dynamics*, vol. 23, no. 3, pp. 249–261, Mar. 2010.